

## Development of flow stress model for hot deformation of Ti–47%Al alloy

DENG Tai-qing, YE Lei, SUN Hong-fei, HU Lian-xi, YUAN Shi-jian

School of Materials Science and Engineering, Harbin Institute of Technology, Harbin 150001, China

Received 10 May 2011; accepted 25 July 2011

**Abstract:** The hot deformation behavior of a  $\gamma$ -TiAl based alloy (Ti–47%Al, mole fraction) was investigated by isothermal compression tests performed at elevated temperature of 900–1200 °C and strain rate of 0.001–0.02 s<sup>-1</sup>. The effect of temperature, strain rate and strain on the flow stress of the alloy was evaluated. The higher the deformation temperature and the lower the strain rate, the smaller the deformation resistance. The stress exponent,  $n$ , and the apparent activation energy,  $Q$ , were determined as 2.6 and 321.2 kJ/mol by the sine hyperbolic law, respectively. Based on the experimental results by the orthogonal method, a flow stress model for hot deformation was established by stepwise regression analysis. Then the effectiveness of the flow stress model was confirmed by other experimental data different from those experimental data used to establish the model. And it was proved that the flow stress model can well predict the mechanical behavior and flow stress of the alloy during hot deformation.

**Key words:**  $\gamma$ -TiAl based alloy; hot compression; flow stress model; deformation behavior

### 1 Introduction

The  $\gamma$ -TiAl based alloys have been considered for high-temperature structural applications due to their high melting-point, high strength retention at elevated temperature, and good thermal stability [1–2]. However, the intrinsic high hardness and low ductility of these alloys at room temperature makes it very difficult to produce components by machining or cutting processing [3–4]. Although, in the past decades, significant progress has been made in the research and development of  $\gamma$ -TiAl based alloys [5–7], the improvement of their room-temperature plasticity and the forming of complicated components are still great challenges. Among the techniques used for forming of  $\gamma$ -TiAl based alloys, the deformation processing route, in particular, the isothermal forging process, is believed to be the most effective way to produce complicated, high-performance components [8–9]. In an effort to optimize the deformation processing process, many recent researches have been focused on the hot deformation behavior of  $\gamma$ -TiAl based alloys [7, 10–12].

With the rapid development of computing techniques, FEM simulation is widely applied to study the metal forming processes [13–14]. Numerical simulation can be truly reliable only when a proper material constitutive model is constructed. Therefore, it is very important to establish the constitutive model, or

the flow stress model which depicts the dependence of flow stress on deformation temperature, strain rate, and strain, in order not only to effectively perform numerical simulation, but also to achieve optimization of the hot forming processes. Indeed, extensive works have been carried out to describe the flow stress as a function of temperature, strain rate, and strain in a number of materials. Modifications to the widely used Johnson-Cook constitutive model were proposed by VURAL and CARD [15]. SLOOFF et al [16], HE et al [17] and PU et al [18] established the constitutive model based on the Arrhenius-type equation and the sine hyperbolic description for the Zener-Hollomon parameter. HE et al [19] and LUO et al [20] constructed the constitutive model by the method of artificial neural network (ANN). HUANG et al [21] applied the regression analysis method to establish the constitutive model.

In this work, an investigation on the hot deformation behavior of a  $\gamma$ -TiAl based alloy (Ti–47%Al, mole fraction) by compression tests, and the establishment and its effectiveness confirmation of the flow stress model for hot deformation of the alloy based on the orthogonal experimental results and the regression analysis were reported.

### 2 Experimental

#### 2.1 High temperature compression experiments

The Ti–47%Al alloy used in the present study was

produced by the elemental powder metallurgy route as shown in Ref. [22]. Cylindrical samples of  $d 6 \text{ mm} \times 9 \text{ mm}$  in size, which were prepared by electric-discharge cutting, were used for the compression tests. The isothermal compression tests were performed on a GLEEBLE 1500D thermal-mechanical simulation machine at elevated temperature of 900–1 200 °C and at a strain rate of 0.001–0.02  $\text{s}^{-1}$ .

## 2.2 Orthogonal experiment design

In this work, the flow stress of the alloy during deformation was selected as the object function, while the temperature, the strain rate, and the strain were selected as the affecting factors. The orthogonal design for the factors and their levels of the isothermal compression tests are shown in Table 1. Based on the consideration of the first-level interaction of affecting

factors and levels, the orthogonal table design of  $L_{18}(3^7)$  was used.

**Table 1** Factors and levels of orthogonal design

Level	Temperatures/°C	Strain rate/ $\text{s}^{-1}$	Strain
1	900	0.001	0.10
2	1 000	0.005	0.25
3	1 100	0.01	0.40

## 3 Results and discussion

### 3.1 True stress—strain curves

The true stress—strain curves of Ti–47%Al alloy obtained by isothermal compression tests at different deformation conditions are shown in Fig. 1. The characteristics of the true stress—strain curves can be

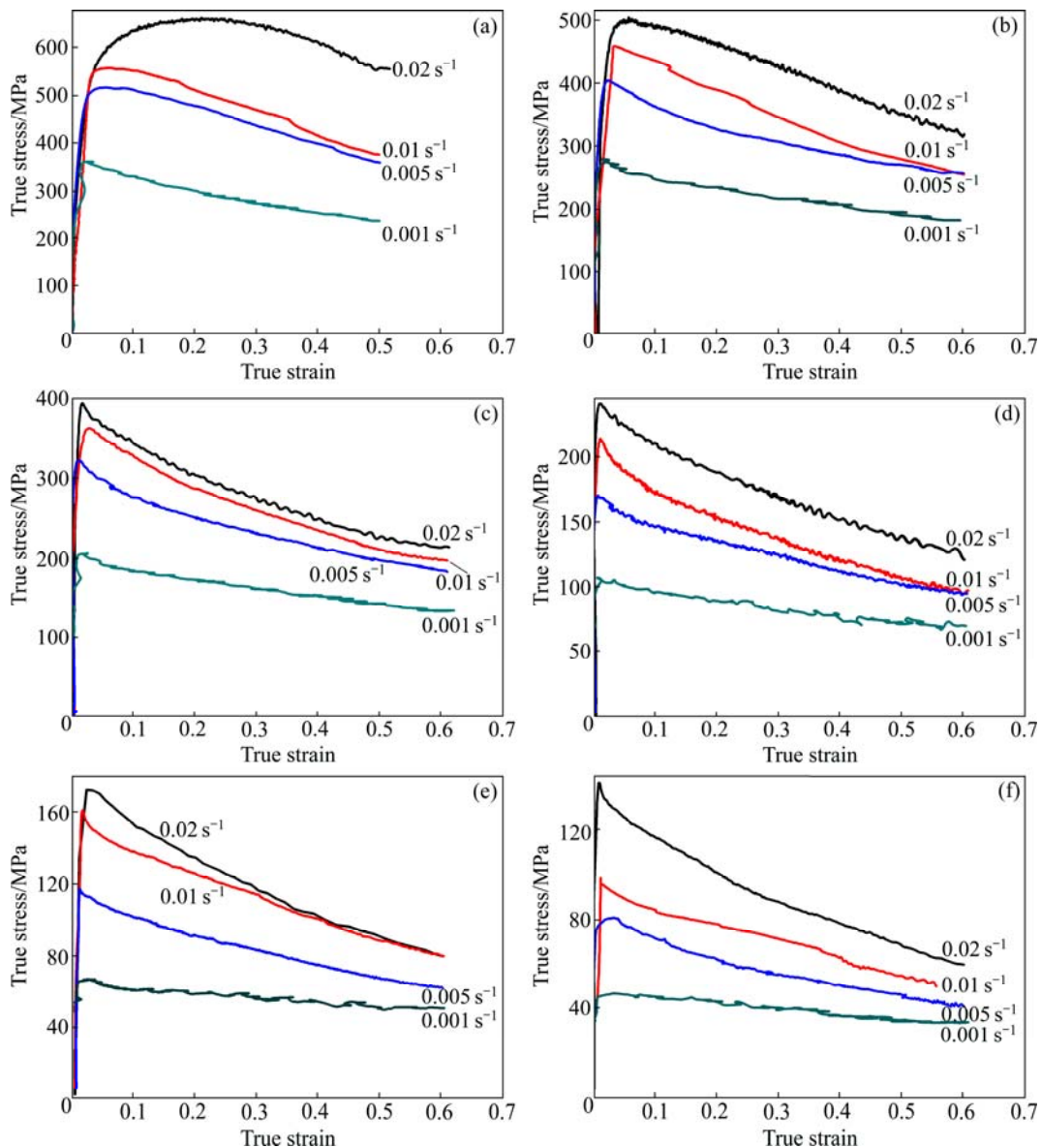


**Fig. 1** True stress—strain curves of Ti–47%Al alloy under different deformation conditions: (a) 900 °C; (b) 950 °C; (c) 1 000 °C; (d) 1 100 °C; (e) 1 150 °C; (f) 1 200 °C

summarized as follows.

1) In general, the flow stress of the alloy at first increases rapidly by work hardening with increasing strain until it achieves its peak value. Then, with the further increase of strain, the flow stress decreases progressively, suggesting that strain softening occurs due to dynamic recrystallization in this later stage of deformation.

2) The flow stress is sensitive to deformation temperature and strain rate. The flow stress decreases significantly with the increase of temperature and the decrease of strain rate. This indicates that the higher the deformation temperature and the lower the strain rate, the smaller the deformation resistance.

3) The flow stress is also strain-dependent. At temperature below 1 150 °C and strain rate higher than 0.005 s<sup>-1</sup>, the flow stress during deformation decreases rapidly with increasing strain after it achieves its peak value. For deformation at temperature above 1 150 °C and strain rate lower than 0.005 s<sup>-1</sup>, the true stress vs true strain curves are nearly flat with increasing strain, suggesting that the flow stress is much less sensitive to the strain.

In Refs. [16–18], it has been shown that the sine hyperbolic description for the Zener-Hollomon parameter can be used for flow stress calculation in the hot working regime. The sine hyperbolic law combines the power law and the exponential law in the low and high stress limit, respectively, resulting in a single expression suitable for analysis over the range of temperatures and strain rates currently investigated. For the present analysis of the hot deformation behavior of the Ti–47%Al alloy, the following sine hyperbolic equation is used:

$$Z = A[\sinh(\alpha\sigma)]^n = \dot{\epsilon} \exp\left(\frac{Q}{RT}\right) \quad (1)$$

where  $Z$  is the Zener-Hollomon parameter,  $A$  and  $n$  are material parameters,  $\alpha$  is the stress multiplier,  $\sigma$  is the flow stress,  $\dot{\epsilon}$  is the strain rate,  $Q$  is the apparent activation energy,  $R$  is the universal gas constant and  $T$  is the thermodynamic temperature. In order to understand the deformation characteristic of the alloy at high temperature, the stress exponent  $n$  and the activation energy of hot deformation  $Q$  are obtained by the following methods. Taking the natural logarithm on both sides of Eq. (1), it follows that:

$$\ln \dot{\epsilon} = \ln A + n \ln [\sinh(\alpha\sigma)] - Q/(RT) \quad (2)$$

By plotting  $\ln[\sinh(\alpha\sigma_p)]$  against  $\ln \dot{\epsilon}$  at different temperatures and fixed strains, and adjusting the stress parameter  $\alpha$ , it is possible to make the plots parallel for all test temperatures. The average inverse slope of the

fitted lines is the stress exponent  $n$ . An example of such a plot is shown in Fig. 2, in which the peak stress  $\sigma_p$  in the stress–strain curves is considered to be the flow stress in  $\ln[\sinh(\alpha\sigma_p)]$ . By this way, the value of  $n$  is figured out to be about 2.6. Rearranging Eq. (2) and differentiating with respect to  $1/T$  gives:

$$Q = Rn \frac{d \ln[\sinh(\alpha\sigma)]}{d(1/T)} \quad (3)$$

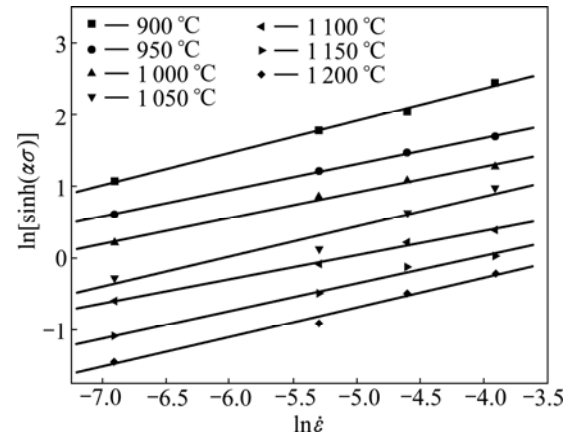
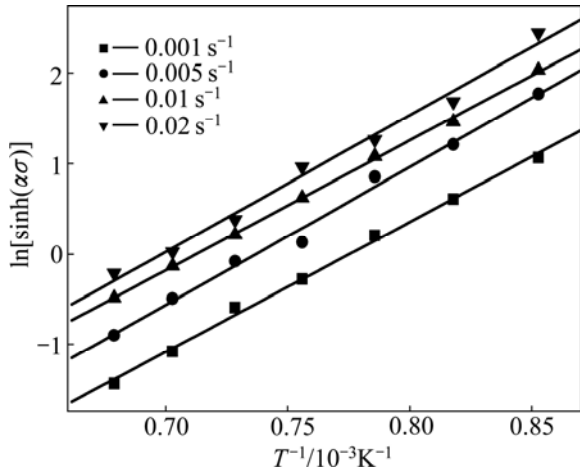


Fig. 2 Relationship between  $\ln[\sinh(\alpha\sigma_p)]$  and  $\ln \dot{\epsilon}$  at different temperatures after optimization of stress multiplier  $\alpha$

Plotting  $\ln[\sinh(\alpha\sigma_p)]$  against  $1/T$  at peak stress  $\sigma_p$  and fixed strain rate, as shown in Fig. 3, gives an average slope  $S$ , which can then be used for calculating the apparent activation energy for deformation, i.e.  $Q = RnS$ . The activation energy for the hot deformation of the currently investigated Ti–47%Al alloy,  $Q$ , is determined to be about 321.2 kJ/mol, which is a little lower than the 366.6 kJ/mol for the Ti–45Al–8.0Nb–0.2B–0.2W–0.02Y alloy, 322.2 kJ/mol for the Ti–46.5Al–2.5V–1Cr and 381 kJ/mol for the Ti–46.5Al–2.5V–1Cr–0.25B alloy, respectively [12, 18]. With the activation energy obtained, the Zener-Hollomon parameter  $Z$  can be calculated using the data available for different strains, strain rates and temperatures and the plot of  $\ln Z$  against  $\ln[\sinh(\alpha\sigma_p)]$  is shown in Fig. 4. It is shown that the points in Fig. 4 fit well with Eq. (1).

### 3.2 Analysis of orthogonal design

The analysis of orthogonal design for the hot compression results is shown in Table 2.  $t_1$ ,  $t_2$  and  $t_3$  are the average flow stresses corresponding to different factors under levels 1, 2, and 3, respectively. The maximum difference between  $t_1$ ,  $t_2$  and  $t_3$  is defined by the symbol “ $R$ ”. The larger the value of  $R$ , the stronger its effect on the objective function is. From Table 2, the order of the seven factors’ effect on flow stress is obtained as follows:  $R_A > R_B > R_C > R_{A \times C} > R_{A \times B} > R_{B \times C}$ .



**Fig. 3** Relationship between  $\ln[\sinh(\alpha\sigma)]$  and  $1/T$  at all strain rates to determine average slope  $S$ , for calculating activation energy

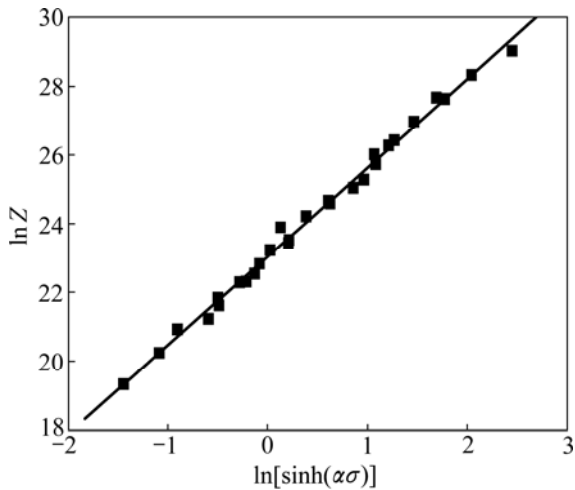


**Fig. 4** Relationship between  $\ln Z$  and  $\ln[\sinh(\alpha\sigma)]$  at investigated temperatures and strain rates

**Table 2** Analysis of orthogonal design

Item	Flow stress/MPa		
	<i>A</i>	<i>B</i>	<i>A</i> × <i>B</i>
$t_1$	409.000	180.667	250.333
$t_2$	234.667	283.167	263.167
$t_3$	118.833	298.667	249.000
<i>R</i>	290.167	118.000	14.167

Item	Flow stress/MPa		
	<i>C</i>	<i>A</i> × <i>C</i>	<i>B</i> × <i>C</i>
$t_1$	284.500	255.500	252.000
$t_2$	267.500	240.833	253.667
$t_3$	210.500	266.167	256.833
<i>R</i>	74.000	25.334	4.833

*A* denotes temperature, °C; *B* denotes strain rate, s<sup>-1</sup>; *C* denotes strain; *A*×*B* denotes first level interaction of *A* and *B*.

Though, as compared with the individual factors, the first level interactions of these factors present much less effect on the value of *R*, such effect is not negligible. So, in this work, the interactions of factors are also considered while constructing the constitutive model by using the multiple linear regression analysis, which is discussed in the following section.

**3.3 Establishment of constitutive equations**

Based on the experimental data of isothermal compression tests, a non-linear constitutive model is constructed by stepwise regression analysis in this work. Such an approach, although it lacks the universal appeal of a mechanical equation of state, has a better chance of adoption by process industries irrespective of detailed understanding of the physics of deformation.

According to the results of orthogonal design and the flow stress—strain curves, the major factors which affect the flow stress including the temperature, the strain rate, the strain and their interactions are considered in the establishment of the constitutive model by stepwise regression for the hot deformation of Ti–47%Al alloy. Table 3 shows that the experimental data are divided into two groups, one is used to construct the model which is defined by the symbol “*C*”, and the other defined by the symbol “*V*” acts as the verification data.

**Table 3** Experimental data of compression tests

Temperature/°C	Strain rate/s <sup>-1</sup>			
	0.001	0.005	0.01	0.02
900	<i>C</i>	<i>V</i>	<i>C</i>	<i>V</i>
950	<i>V</i>	<i>C</i>	<i>V</i>	<i>C</i>
1 000	<i>C</i>	<i>V</i>	<i>C</i>	<i>V</i>
1 050	<i>V</i>	<i>C</i>	<i>V</i>	<i>C</i>
1 100	<i>C</i>	<i>V</i>	<i>C</i>	<i>V</i>
1 150	<i>V</i>	<i>C</i>	<i>V</i>	<i>C</i>
1 200	<i>C</i>	<i>V</i>	<i>C</i>	<i>V</i>

Then, the constitutive model is described in terms of the following equation:

$$y = \beta_0 + \beta_1 x_1 + \beta_2 x_2 + \dots + \beta_9 x_9 \tag{4}$$

where *y* stands for  $\ln \sigma$ , while  $x_1, x_2, \dots, x_9$  are  $1\ 000/T$ ,  $\ln \dot{\epsilon}, \epsilon, (1\ 000/T)^2, (\ln \dot{\epsilon})^2, \epsilon^2, \ln \dot{\epsilon} \times (1\ 000/T), \epsilon \times 1\ 000/T, \ln \dot{\epsilon} \times \epsilon$ , respectively.  $\beta_0, \beta_1, \dots, \beta_9$  are the coefficients of regression equation.

In statistics, stepwise regression includes regression models in which the choice of predictive variables is carried out by an automatic procedure [23]. Based on the constructing data, the flow stress model, or the constitutive equation, for the hot deformation of

Ti–47%Al alloy is obtained as follows:

$$\ln \sigma = -1.669 + 10.916 \times 1000 / T + 0.248 \ln \dot{\varepsilon} - 0.913 \varepsilon \quad (5)$$

### 3.4 Verification and evaluation for model

The results of analysis of variance (ANOVA) of the regression equation are presented in Table 4. In order to make sure that the established constitutive model is reasonable,  $F$ -test of statistics is used in this work. Since, as shown in Table 4, the value of  $F$  is 277.479, which is much greater than the value of  $F_{0.01}(3, 23)$  reported to be 4.76 [23], and the multiple correlation coefficient is 0.986, it is obvious that the dependent variable has a highly regression relationship with the independent variables.

In order to evaluate the accuracy of strain–stress relationship shown in Eq. (5), an error analysis was carried out for different strain levels. The data  $C$  and  $V$  are used to check the accuracy of the equation developed in the above section, with the results of the analysis shown in Fig. 5. It clearly demonstrates that most of the calculated data agree well with the experimental data. The deviations between the experimental and the calculated flow stresses at different strain levels are determined using the following form:

$$D = \frac{|\sigma_C - \sigma_E|}{\sigma_C} \times 100\% \quad (6)$$

where  $\sigma_C$  is the calculated value of the flow stress and  $\sigma_E$  is the experimental value of the flow stress.

The correlation coefficient between the calculations by Eq. (5) and the experimental data  $C$  is 0.987 79, with mean deviation of 7.04%, and the correlation coefficient between the calculations and the experimental data  $V$  is 0.985 16, with mean deviation of 8.72%, respectively. The deviation analysis shows that the constitutive relationship established in this work can well describe the flow stress of the Ti–47%Al alloy at different strain rates, deformation temperatures, and strain levels.

In order to confirm the validity of the flow stress model represented by Eq. (5), the flow stresses at different deformation conditions are calculated by Eq. (5) and compared with both the experimental data  $C$  and the data  $V$ , as shown in Fig. 6 and Fig. 7, respectively. This further shows that the established flow stress model can well describe the flow stress of the Ti–47%Al alloy

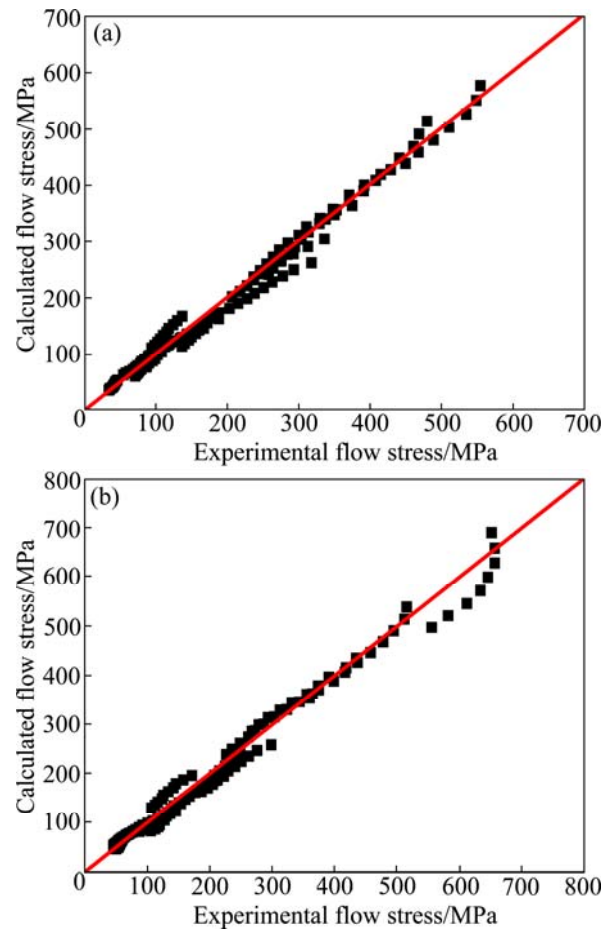


**Fig. 5** Comparison of calculated and experimental flow stress values at different temperatures and stain rates: (a) Comparison of calculations and experimental data  $C$ ; (b) Comparison of calculations and experimental data  $V$

during hot deformation at different temperatures, strain rates and strains under the conditions investigated in this work.

## 4 Conclusions

1) The flow stress is significantly affected by deformation temperature and strain rate during hot deformation. The higher the deformation temperature and the lower the strain rate, the smaller the deformation resistance.

2) The material parameters, stress exponent  $n$  and the apparent activation energy  $Q$ , are determined as 2.6

**Table 4** Analysis of variance (ANOVA)

Variance	Sum of squares	Freedom	Mean square deviation	$F$	Significant level $\alpha$	Multiple correlation coefficient
SSR	13.028	3	4.343			
SSE	0.36	23	0.016	277.479	0	0.986
SST	13.388	26				

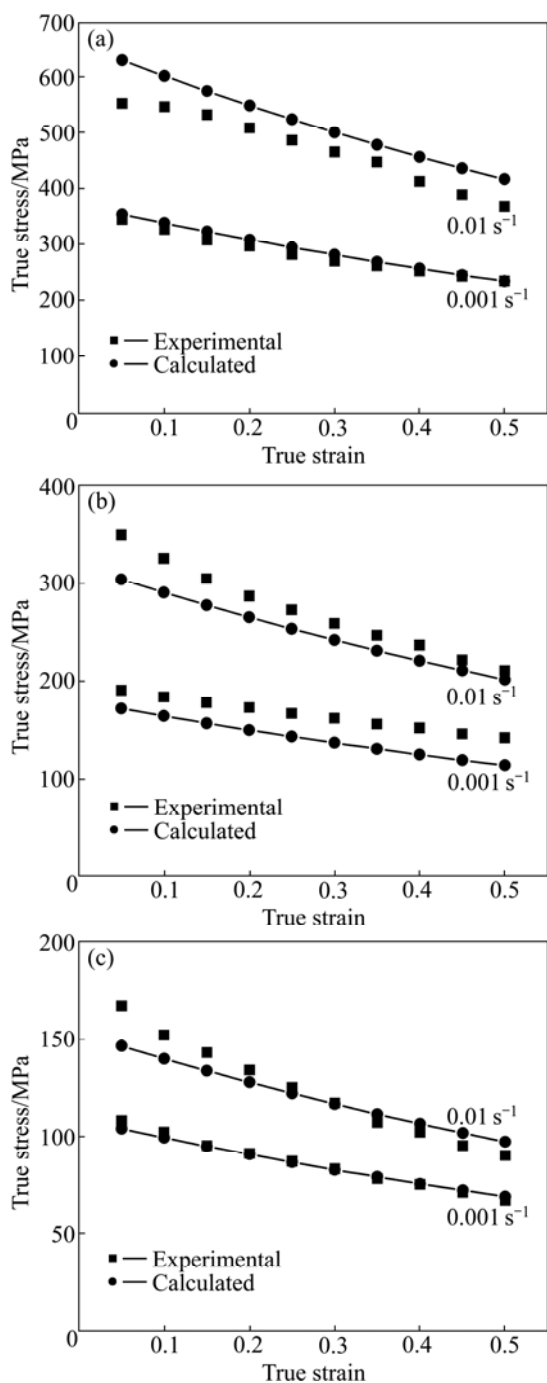


**Fig. 6** Comparison of flow stresses calculated by Eq. (5) and experimental data  $C$  at different deformation conditions: (a) 900 °C; (b) 1 000 °C; (c) 1 150 °C

and 321.2 kJ/mol by sine hyperbolic law, respectively.

3) The flow stress of the Ti-47%Al alloy is sensitive to deformation temperature and strain rate, the strain also has a significant influence on the flow stress.

4) The constitutive model is constructed by stepwise regression as follows:

$$\ln \sigma = -1.669 + 10.916 \times 1000/T + 0.248 \ln \dot{\epsilon} - 0.913 \epsilon$$

5) The results of verification for constitutive model indicate that the proposed material constitutive model

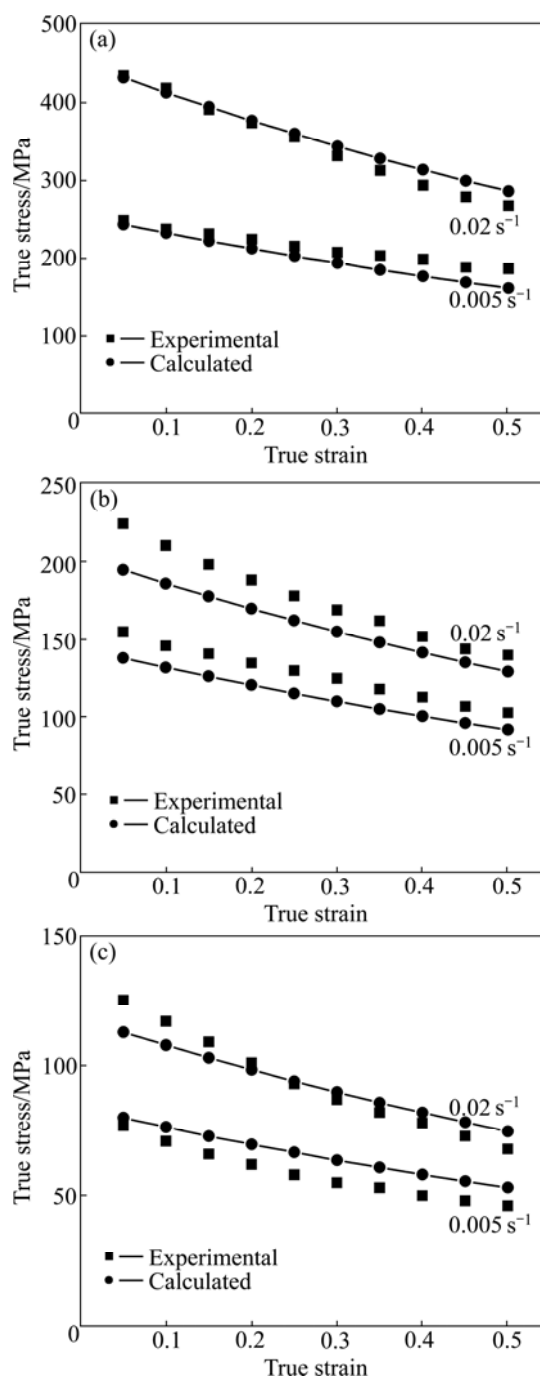


**Fig. 7** Comparison of flow stresses calculated by Eq. (5) and experimental data  $V$  at different deformation conditions: (a) 950 °C; (b) 1 100 °C; (c) 1 200 °C

can properly describe and predict the flow stress of Ti-47%Al alloy in the range of temperature  $T > 900$  °C and strain rate  $\dot{\epsilon} < 0.02$  s<sup>-1</sup>.

## References

- [1] KIM Y M. Ordered intermetallic alloys: Part III. Gamma titanium aluminides [J]. JOM, 1994, 46: 30–39.
- [2] EDWARD A. Gamma titanium aluminides as prospective structural materials [J]. Intermetallics, 2000, 8: 1339–1345.

- [3] KIM Y W. Strength and ductility in TiAl alloys [J]. *Intermetallics*, 1998, 6: 623–628.
- [4] THOMAS M, RAVIART J L, POPOFF F. Cast and PM processing development in gamma aluminides [J]. *Intermetallics*, 2005, 13: 944–951.
- [5] KIM Y W. Microstructure evolution and mechanical properties of a forged gamma titanium aluminide alloy [J]. *Acta Metall Mater*, 1992, 40: 1121–1134.
- [6] LIU C T, MAZIASZ P J. Microstructural control and mechanical properties of dual-phase TiAl alloys [J]. *Intermetallics*, 1998, 6: 653–661.
- [7] HUANG Z H. Workability and microstructure evolution of Ti-47Al-2Cr-1Nb alloy during isothermal deformation [J]. *Intermetallics*, 2005, 13: 245–250.
- [8] APPEL F, BROSSMAN U, CHRISTOPH U, EGGERT S, LORENZ U. Recent progress in the development of gamma titanium aluminide alloys [J]. *Adv Eng Mater*, 2000, 2: 699–720.
- [9] APPEL F, OEHRINGA M, PAULA D H, CARNEIROC T. Physical aspects of hot-working gamma-based titanium aluminides [J]. *Intermetallics*, 2004, 12: 791–802.
- [10] LIN J P, XU X J, WANG Y L, HE S F, ZHANG Y, SONG X P, CHEN G L. High temperature deformation behaviors of a high Nb containing TiAl alloy [J]. *Intermetallics*, 2007, 15: 668–674.
- [11] HUANG J S, HUANG L, LIU B, ZHANG Y H, ZHANG W, HE X Y, LIU Y. Simulation of hot compression of Ti-Al alloy [J]. *Intermetallics*, 2007, 15: 700–705.
- [12] LI S S, SU X K, HAN Y F, XU X J, CHEN G L. Simulation of hot deformation of TiAl based alloy containing high Nb [J]. *Intermetallics*, 2005, 13: 323–328.
- [13] DAVIM J P, MARANHAO C. A study of plastic strain and plastic strain rate in machining of steel AISI 1045 using FEM analysis [J]. *Materials and Design*, 2009, 30: 162.
- [14] MADALINA C, DOMINIQUE C, FRANK G. A new material model for 2D numerical simulation of serrated chip formation when machining titanium alloy Ti-6Al-4V [J]. *International Journal of Machine Tools & Manufacture*, 2008, 48: 275–288.
- [15] VURAL M, CARO J. Experimental analysis and constitutive modeling for the newly developed 2139-T8 alloy [J]. *Materials Science and Engineering A*, 2009, 520: 56–65.
- [16] SLOOFF F A, ZHOU J, DUSZCZYK J, KATGERMAN L. Constitutive analysis of wrought magnesium alloy Mg-Al4-Zn1 [J]. *Scripta Materialia*, 2007, 57: 759–762.
- [17] HE Xiao-ming, YU Zhong-qi, LIU Gui-ming, WANG Wen-ge, LAI Xin-min. Mathematical modeling for high temperature flow behavior of as-cast Ti-45Al-8.5Nb-(W,B,Y) alloy [J]. *Materials and Design*, 2009, 30: 166–169.
- [18] PU Z J, WU K H, SHI J, ZOU D. Development of constitutive relationships for the hot deformation of boron microalloying TiAl-Cr-V alloys [J]. *Materials Science and Engineering A*, 1995, 192–193: 783–785.
- [19] HE Xiao-ming, YU Zhong-qi, LAI Xin-min. Analysis of high temperature deformation behavior of a high Nb containing TiAl based alloy [J]. *Mater Letters*, 2008, 62: 4181–4183.
- [20] LUO Jiao, LI Miao-quan, HU Yi-qu, FU M W. Modeling of constitutive relationships and microstructural variables of Ti-6.62Al-5.14Sn-1.82Zr alloy during high temperature deformation [J]. *Materials Characterization*, 2008, 59(10): 1386–1394.
- [21] HUANG C, DEAN T A, LORETTO M H. Deformation behaviour of Ti-25Al-10Nb-3V-1Mo (supper  $\alpha_2$ ) during isothermal forging [J]. *Materials Science and Engineering A*, 1996, 208: 166–177.
- [22] FANG Wen-bin, HU Lian-xi, HE Wen-xiong, WANG Er-de, LI Xiao-qing. Microstructure and properties of a TiAl alloy prepared by mechanical milling and subsequent reactive sintering [J]. *Materials Science and Engineering A*, 2005, 403: 186–190.
- [23] XIAO Qun, LIU Wen-qing. *Applied regression analysis* [M]. Beijing: China Renmin University Press, 2001: 345. (in Chinese)

## Ti-47%Al 合金在热变形下的流动应力本构模型

邓太庆, 叶磊, 孙宏飞, 胡连喜, 苑世剑

哈尔滨工业大学 材料科学与工程学院, 哈尔滨 150001

**摘要:** 通过等温压缩试验, 对  $\gamma$ -TiAl 基合金(Ti-47%Al 合金, 摩尔分数)在温度为 900~1 200 °C 和应变速率为 0.001~0.02 s<sup>-1</sup> 条件下的变形行为进行研究。研究发现, 变形温度、应变速率和应变对该合金的流动应力有很大影响, 变形温度越高, 应变速率越小, 流动应力就越小。利用双曲正弦方程求得该合金的应力指数  $n$  为 2.6 和激活能  $Q$  为 321.2 kJ/mol。运用逐步回归的方法, 建立该合金的流动应力模型, 并用实验数据对该模型进行评估和验证。表明提出的模型能很好地用来预测该合金在热变形过程中的流动应力和力学性能。

**关键词:**  $\gamma$ -TiAl 基合金; 热压缩; 流动应力模型; 变形行为

(Edited by YANG You-ping)